Computational Eco-Systems for Handwritten Digits Recognition

A. Loquercio[a,b,*], F. Della Torre[a], M. Buscema[a,c]

[a] *Semeion Centro Ricerche di Scienza della Comunicazione, Via Sersale 117, 00128 Roma*
[b] *Robotics and Perception Group, University of Zurich, Andreastrasse 15, 8050 Zurich*
[c] *Department of Mathematical and Statistical Sciences, CCMB, University of Colorado, P.O. Box 173364, Denver, CO 80217, USA*

Abstract

On tasks such as the recognition of handwritten digits, traditional methods from machine learning and computer vision have always failed to beat human performance. Inspired by the importance of diversity in biological system, we built an heterogeneous system that could achieve this goal. Our architecture could be summarized in two basic steps. First, we generate a diverse set of classification hypothesis using both Convolutional Neural Networks, currently the state-of-the-art technique for this task, among with other traditional and innovative machine learning techniques. Then, we optimally combine them through Meta-Nets, a family of recently developed and performing ensemble methods. In the resulting parliament of classifiers all hypothesis, despite of their accuracy or methodology, are considered. On the very competitive MNIST handwriting benchmark, our method is the first to beat human performance with 0.17% error rate, surprisingly showing diversity to be the key for success in decision making.

Keywords: Image Preprocessing, Deep Neural Networks, Image Classification, Meta-Nets, Digit Recognition

1. Introduction

Even though the process of identifying a visual concept in an image is relatively trivial for a human, it involves several challenges from an algorithmic viewpoint. For example, deformations, occlusions, and strong intra-class variation usually make impossible to algorithmically specify a classification rule.

After the introduction of Convolutional Neural Networks (CNNs), systems aimed to this task had a considerable boost in performance. Instead, traditional shallow networks usually do not perform extremely well in image classification when trained on

*Corresponding author
Email addresses: loquercio@ifi.uzh.ch (A. Loquercio), m.buscema@semeion.it (M. Buscema)
URL: http://www.semeion.it (M. Buscema)

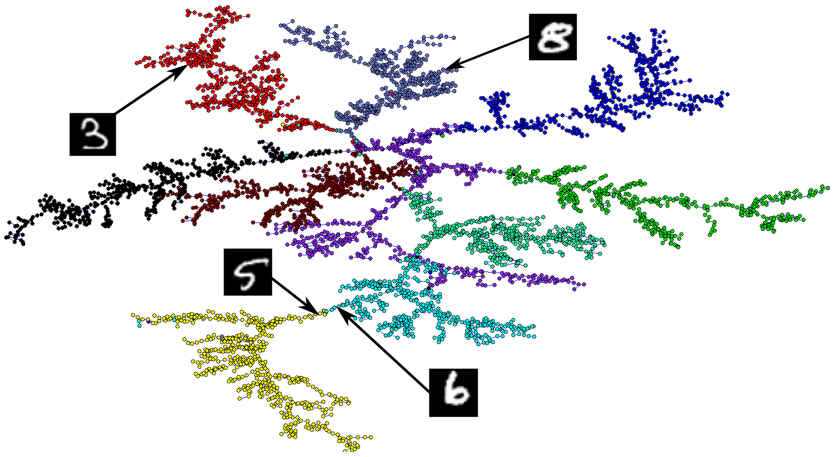

Figure 1: **Samples map.** The classification methodologies herein proposed not only increases accuracy with respect to classical methods, but also include visualization tools. In this figure, we present similarities between the test samples of the MNIST dataset, in the form of a minimum spanning tree. Each node is a sample transformed with one of our classifier (K-CM), whilst each color is associated to a different digit. Apart from the very good clustering, we can see that similarly shaped, but distinct, digits are close in the graph.

raw data [1]. The main reason is their incapacity to learn the invariance to affine deformations and intra-class variations that makes CNNs so powerful [2]. To cope against this problem, we will extract feature maps from our CNNs, and use them to more efficiently train our shallow networks.

In fact, convinced by the importance of both deep and shallow networks, we built a computational ecosystem whose main strength is the ability to combine them. This will be accomplished through Meta-Nets [3], a family of unsupervised ensemble methods. The resulting classification rule, independent by the type of networks and consisting in an optimal weighting of decisions, achieves astonishing results, even beating human performance.

Surprisingly, we noticed that less accurate classification hypothesis are in particular necessary to produce a performing prediction rule, therefore demonstrating the importance of diversity in decision making.

In conclusion, the system we propose herein will also generate a visual understanding of the classifier's behaviour by creating similarity maps between samples, as shown in Fig. 1, or between system components, as shown in Fig. 4. This allows to make more transparent our decision making, usually considered to be a black-box.

Overall, this work makes the following contributions:

- We use CNNs as both classifiers and feature extractors, making their robustness available to a set of well known and innovative supervised shallow networks.
- We employ Meta-Net, an unsupervised ensemble algorithm, to optimally combine decisions from CNNs and other classification methods, despite their differences in learning strategy and topology.

- We propose a new way to visualize a classifier decision making process by generating a set of representative maps, hence clarifying its behaviour.
- We demonstrate the effectiveness of our methods by providing a new state-of-the-art result for the very competitive MNIST dataset.

2. Related Work

Very deep networks have proved to achieve impressive results on various image classification benchmarks [4]. Unlike many others computer vision techniques, CNNs combine both *feature extraction* and *classification*. This is basically pursued by gradient descent techniques, aimed at optimizing a pre-defined cost function.

Other pipelines deploy only the *feature extraction* part of the CNN architecture, using one of its last layers as image descriptor [5, 6]. This technique has successful applications not limited to classification, but also extending to object detection, patch retrieval, and stereo matching [7, 6, 8]. For this reason, we used CNNs feature maps as input to a great variety of shallow learning algorithms. Surprisingly, with this approach it is even possible to beat the performance of the CNN used to extract features, as long as their learning policy is much different from the one used by the *father* CNN.

However, since diversity represents a key component of many biological and computational systems [9], we aimed to generate a robust classification rule by combining both deep and shallow networks' predictions. A similar idea can be found in [2], where multiple hypothesis are built by training several CNNs on augmented partitions of the original dataset. Majority vote is eventually used to produce a final classification label. Even if they achieved very good results, we believe their limited classification diversity and the simplicity of their ensemble method to pose serious limits on performance.

In the literature, it is possible to find several methods to construct performing ensembles, going from supervised methods, as bagging [10], to unsupervised ones, as GUACAMOLE [11]. One of the most famous and performing algorithms in this area is AdaBoost [12], which manipulates the training set to generate multiple hypothesis. The final classifier is determined by a weighted vote of the individual classifiers, with the weight being a function of its accuracy.

Similarly to AdaBoost, the ensemble method we use in our experiments makes decisions by a weighted average of the individual classifiers. Differently from AdaBoost, the weight is a function of the classifier confusion matrix on validation data, no assumption is made on the base classifiers, and no training set manipulations during learning are required. Our system, called Meta-Net, proves to improve on others ensemble types [3], and it is able to both use the advantages of supervision, and to employ the competitive learning structure typical of unsupervised methods [11].

In conclusion, we will present a novel technique to generate a visual understanding of the system decision making process. Since the learned features of CNNs are not interpretable, understanding and visualizing their inner mechanisms is a difficult task. Nonetheless, in the literature there are some solutions to this problem, as retrieving images that maximally activate a neuron [13], down-projecting feature maps to a 2 or 3 dimensional space, or generating heatmaps to reveal CNNs' region of interest for classification [14].

CNN	0	1	2	3	4	5	6
Pre-processing	None	None	None	None	None	Crop(2,2)	Crop(2,2)
Conv-(4,4,20)	✓	✓	✓	✓	✓	✓	✓
Avg-pool-(2,2)	✓	✓	✓	✓	✓	✓	✓
Conv-(5,5,40)	✓	✓	✓	✓	✓	✓	✓
Avg-pool-(3,3)	✓	✓	✓	✓	✓	✓	✓
Conv-(2,2,32)	✗	✓	✓	✗	✗	✓	✓
Avg-pool-(2,2)	✗	✓	✓	✗	✗	✓	✓
Dense	150	150	150	150	128	✗	150
Data-Augment.	✗	✓	✓	✓	✓	✓	✓
Activation	relu	elu	relu	relu	relu	relu	relu

Table 1: **CNNs committee**. The above table reports the details of the CNNs used in the experiments. Their last hidden layer is used as descriptor for input images after training. To decrease over-fitting, a dropout layer is used after each pooling or dense layer. Moreover Data-Augmentation on the training set is employed to increase the CNNs robustness.

With our system we are able to visually appreciate samples similarities, avoiding the lossly down-projection step, and through the simple graph structure of a tree, as shown in Fig. 1. Moreover, we will present an other graph to highlight the correlations between classification hypothesis, giving insights on the relationship and differences of their decision making process. To our knowledge, this technique is still unexplored in the literature.

3. Methodology

Fig. 2 summarizes our methodology. First, we trained a committee of seven different CNNs, whose details are shown in Table 1. Then, apart from being used as classifiers, we employed them also as robust feature extractors. In fact, we produced for each image a descriptor consisting in the last hidden layer of a CNN. Different deep networks will therefore produce distinct encoding of the same dataset. The latter representations will then be given as input to a set of traditional and innovative classification algorithms, aiming to generate a great *Computational Bio-diversity*, where each method produces distinct classification hypothesis. The generated predictions are eventually combined through Meta-Net [3], to fully exploit all the available *biodiversity* in the base classifiers. The underlying intuition is that, as in biological systems, diversity is the key for success in decision making.

The remainder of this section will present our methods in detail. In the following we will first introduce the set of our base classifiers, then review the basics of Meta-Net, our ensemble building method. Eventually, we will present our graph-visualization tool used to give insights into the way our methods behave.

3.1. Supervised classifiers

In our experiments we use both well-known traditional methods as well as more recent and innovative classifiers from the literature. We chose to use: AVQ [15], [16], [17] and [18], Bayes Net [19] and [20], BP [21] and [22], CNN [1], KNN [23], [24]

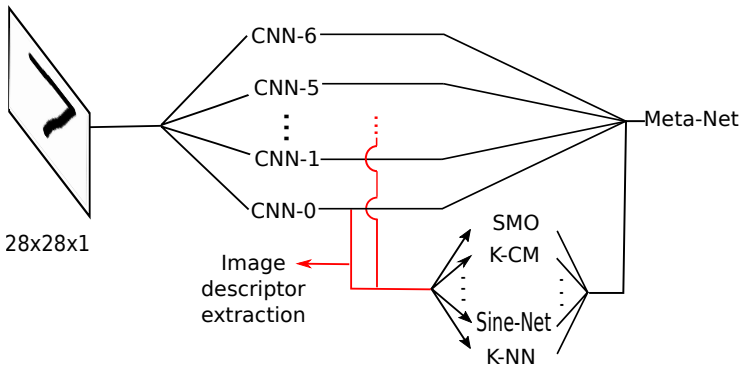

Figure 2: **Methodology**: The proposed systems builds a robust prediction rule by combining two types of classifiers: CNNs, currently the state-of-the-art technique for image classification, and traditional shallow classifiers from the literature. To give the latter more robustness to photometric changes, we trained them using the last hidden layers of some CNNs as image descriptors. The resultant hypothesis will be then combined with Meta-Nets [3], a set of very performing ensemble methods.

and [25], Logistic Regression [26] and [27], Naïve Bayes [28], [29] and [30], Random Forest [31] and [32], SMO [33], [34], [35] and [36].

In addiction we use the following algorithms designed at Semeion Research Center: BiModal [37], ConicNet [38], GaussNet [39], K-CM [40] and [41], New Recirculation Neural Network [42], Sine-Net [43], [44] and [45].

In each of the following experiments, different subsets of all these methods are used for classification. More details about them can be found in the appendix.

3.2. Meta-Nets

Meta-Nets[3] is a family of unsupervised ensemble methods, combining the hypothesis coming from many different base classifiers to produce a powerful prediction rule. Each member of this family can be understood as a single layer perceptron, whose weights are established without gradient based methodologies. Their input layer $\mathbf{I}$ consists in the concatenation of the class probabilities produced by each of the classifiers in the ensemble. The output nodes represent instead the final, not normalized, categorical distribution over classes, used for prediction.

Therefore, using K classifiers for a N-classes problem, we have $K \times N$ input nodes and N outputs one. The resulting weight matrix W, of dimensions $N \times (K \times N)$, is generated by a fuzzy function of the sensitivity and precision of each of the base classifiers, as estimated by their confusion matrices on the training set. In particular, defining $a^k_{i,j}$ as the i,j entry of the k^{th} classifier's confusion matrix, we have $W_{k*i,j} = f(S^k_{i,j}, P^k_{i,j})$, where $S^k_{i,j} = a^k_{i,j} / \sum_j^N a^k_{i,j}$ and $P^k_{i,j} = a^k_{i,j} / \sum_i^N a^k_{i,j}$. Eventually, the N-dimensional output $\mathbf{O}$ is then generated as:

$$\mathbf{O} = \mathbf{W} \cdot \mathbf{I} \tag{1}$$

$$WinnerClass = \arg\max_i \{O_i\} \tag{2}$$

Meta-Net	Equation
Meta-Bayes	$W_{k*i,j} = -\ln\left(\frac{(1-S^k_{i,j})\cdot(1-P^k_{i,j})}{S^k_{i,j}\cdot P^k_{i,j}}\right)$
Meta-Sum	$W_{k*i,j} = \frac{1}{2}\left[(S^k_{i,j}+P^k_{i,j}) - (1-S^k_{i,j})\cdot(1-P^k_{i,j})\right]$
Meta-Fuzzy	$W_{k*i,j} = \min\left\{S^k_{i,j}, P^k_{i,j}\right\}$
Meta-Expn	$W_{k*i,j} = \frac{e^{(S^k_{i,j}+P^k_{i,j})}}{e^{(1-S^k_{i,j})\cdot(1-P^k_{i,j})}}$
Meta-Einstein	$W_{k*i,j} = \frac{(S^k_{i,j}+P^k_{i,j})}{1+(1-S^k_{i,j})\cdot(1-P^k_{i,j})}$
Meta-Consensus	$W_{k*i,j} = -\ln\left(\frac{m^k_{i,j}\cdot f^k_{i,j}}{r^k_{i,j}\cdot c^k_{i,j}}\right)$ (see [3] for details)

Table 2: **The Meta-Nets family**

Though all Meta-Nets share this same structure, they employ different activations f in the weights equations. Their characteristics are summarized in Table 2.

We mainly decided to use Meta-Nets because of their independence from the base classifiers' methodology, and of their proved capacity to take advantage of the ensemble's *diversity*. In our experiments, we will in fact show that the higher the difference among classifiers', the better will be the performance. However, not all members of an ensemble might be useful for the final classification rule. Hence, to increase accuracy while decreasing prediction time, we employed the genetic algorithm GenD [46] to determine the subset of base classifiers that produces the best result.

3.3. Network graph

We present two different methods to visualize information on our decision making process. The first one represents the relationship between data samples, while the second one synthesizes the similarity among classifiers.

The semantic K-CM map. The main characteristics of one of our base classifiers, K-CM [40], is its ability to map samples in a space where Euclidean similarities are directly correlated to semantic ones. This mapping, defined Z transform, is built on the base of Auto-CM [47], from which it inherits its contractive properties. The distance between all transformed samples, defined *Meta-Distance* matrix, is used as a weight matrix to compute a Minimum Spanning Tree (MST). In fact, an MST enables us to visually analyze the classifier's belief on samples similarities, as shown in Fig. 1.

The Meta-Net MRG. In order to understand the decision making process of our system, we derived a way to understand which classifiers or meta-classifiers exhibit similar behavior. Using the same procedure as above, we first calculated a semantic *distance* between classifiers, and then visualized the resultant weight matrix through a graph.

The equation used to encode similarities is directly related to the number of common mistakes, and is defined as:

$$D_{i,j} = 2 \cdot \frac{(E_i \wedge E_j)}{E_i + E_j} \cdot \frac{N}{R} \cdot \left(1 - \frac{1}{N}\right) \tag{3}$$

where E_i represents the number of i classifier's error, $E_i \wedge E_j$ the common mistakes between i and j, N the number of classes, and R the number of samples. Eventually, to visualize the classifier's similarities, we computed the *MRG* [47] on the resultant distance matrix. The use of the *MRG* is now preferred because of its property to represent strong similarities, inevitably discarded by a simple MST. In fact, as we can observe in Fig. 4, highly similar classifiers are connected through a clique sub-graph.

4. Experiments

We benchmark our system on the commonly used public dataset MNIST, achieving astonishing results when compared to other published systems.

4.1. Experimental Setup

Following the instructions of the authors, we divided the MNIST dataset in training and testing set, of $60K$ and $10K$ samples respectively. However, we randomly divided the training set into two splits of $50K$ and $10K$ samples. The former is actually used for training, while the latter for validation, *i.e.* to pick the best model up during learning.

Each component of the CNNs committee described in the previous section was trained for 100 epochs with an exponential learning rate. On average, the training of a CNN requires almost an hour on our single NVIDIA GeForce GT 730M. The shallow algorithms have instead varying training times. We calculated that on average, each of them requires 10 minutes to learn.

The machine learning software Tensorflow has been used for training and evaluating the CNNs. Most of the supervised networks and the Meta-Nets, were instead trained with the Semeion software suite "Meta Net Multi Train v3.5"[1]. Few shallow networks were eventually learned using the software Weka.

4.2. Experiments

To prove our thesis we ran a set of four experiments, incrementally increasing the diversity of classification hypothesis and, consequently, the system complexity.

Exp. I. In the first experiment we tested the generalization's ability of the CNNs committee only. Even if the performance of the committee is superior to any of its members, we do not reach any interesting result, as shown in Table 3. The lack of "biodiversity" is in fact the main reason why our ensemble method is beaten by simple averaging, therefore confirming the findings of [2].

[1] Version is 3.5.55, 1999-2017. This software suite is freely available for academic research purposes, and can be obtained by contacting the authors.

Algorithm	Accuracy	Classifiers used
Major Vote	**0.9975**	**all**
Meta-Bayes	**0.9974**	**all**
Meta-Consensus	**0.9973**	**all**
Meta-Einstein	**0.9973**	**all**
Meta-Expn	**0.9973**	**all**
Meta-Fuzzy	**0.9973**	**all**
Meta-Sum	**0.9973**	**all**
CNN2	0.9968	-
CNN6	0.9967	-
CNN1	0.9963	-
CNN5	0.9962	-
CNN4	0.9959	-
CNN0	0.9958	-
CNN3	0.9936	-

Table 3: Experiment I: Ensembles built from the CNNs committee only.

Algorithm	Accuracy	Classifiers Used
Meta-Einstein	**0.9978**	**6**
Meta-Fuzzy	**0.9978**	**6**
Meta-Sum	**0.9978**	**6**
Meta-Bayes	**0.9978**	**8**
Meta-Consensus	**0.9977**	**5**
Major Vote	**0.9972**	**all**
RandomForest	0.9969	-
BackProp(64)	0.9969	-
Bi-Modal(48)	0.9968	-
CNN2	0.9968	-
SMO	0.9967	-
Conic(64)	0.9965	-
GaussNet(120)	0.9963	-
AVQ-Base(36)	0.9962	-
SVCm(36)	0.9962	-
K-CM(5)	0.9961	-

Table 4: Experiment II: Ensembles of a single CNN, and 18 shallow classifiers trained on its features maps. The top ten performing classifiers are shown alongside the ensemble methods. The last column indicates the number of base classifiers, either deep of shallow, used to build the ensembles.

Algorithm	Accuracy	Classifiers used
Meta-Expn	**0.998**	**7**
Meta-Bayes	**0.9979**	**10**
Meta-Consensus	**0.9979**	**6**
Meta-Einstein	**0.9979**	**8**
Meta-Fuzzy	**0.9979**	**11**
Meta-Sum	**0.9979**	**11**
Major Vote	**0.997**	**all**
RandomForest	0.9969	-
BackProp(64)	0.9969	-
Bi-Modal(48)	0.9968	-
CNN2	0.9968	-
SMO	0.9967	-
CNN6	0.9967	-
Conic(64)	0.9965	-
CNN1	0.9963	-
CNN5	0.9962	-
K-CM(5)	0.9961	-

Table 5: Experiment III: Ensembles of 7 CNNs and 9 shallow classifiers trained with features maps extracted from *CNN2* only. The top ten performing classifiers are shown alongside the ensemble methods. The last column indicates the number of base classifiers, either deep of shallow, used to build the ensembles.

Algorithm	Accuracy	Classifiers used
Meta-Einstein	**0.9983**	**11**
Meta-Sum	**0.9983**	**11**
Meta-Bayes	**0.9982**	**16**
Meta-Consensus	**0.9982**	**11**
Meta-Expn	**0.998**	**16**
Meta-Fuzzy	**0.998**	**13**
(2)RandomForest	0.9969	-
(2)Backprop(64)	0.9969	-
(2)BiModal(48)	0.9968	-
CNN2	0.9968	-
(2)SMO	0.9967	-
CNN6	0.9967	-
(2)Conic(64)	0.9965	-
CNN1	0.9963	-
CNN5	0.9962	-
(0)GaussNet(120)	0.9961	-
MajorVote	**0.996**	**all**

Table 6: Experiment IV: Ensembles of 7 CNNs and 50 *children* classifiers, trained with features maps extracted from *CNN0*, *CNN2*, *CNN3*, and *CNN4*. Only the top ten networks and the resulting ensembles are shown. The last column indicates the number of base classifiers, either deep of shallow, used to build the ensembles.

Exp. II. In this second experiment, we investigated the strength of the union between a single CNN and a set of 18 traditional classifiers trained on its last hidden layer. From Table 4 emerges that a concise boost in performance can be obtained through this simple modification. In fact, the best of the generated ensembles, *i.e.* Meta-Einstein, has an error rate of 0.22%, approximately 30% smaller of the corresponding CNN. Moreover, it is interesting to see that some classifiers have an error rate smaller than the deep network used to provide them with input image descriptors. For example, Table 4 shows that the Random Forest algorithm has slightly higher performance (0.01%) than *CNN2*. Even if the small improvement might not be worth the effort, it is still interesting to see that the learned final perceptron step in a CNN can be beaten by a traditional classification algorithm. This is probably due to the highly non-linear manifold where the CNN's feature maps lye.

Exp. III. In this experiments, we deployed the full CNNs committee alongside a set of 10 traditional classifiers trained on the feature maps of *CNN2* only. Their results are reported in Table 5, where we notice that the generated ensembles have already enough diversity to properly generalize. Surprisingly, this simple method already improves state-of-the-art on MNIST with an error rate of 0.20%, despite being much simpler and faster than the previous best system [48].

Exp. IV. To test the role of diversity, in this experiment we increased the number of traditional classifiers. Now, 4 out of 7 CNNs are used to extract image representations. These are then employed to train a total of 50 *shallow* classifiers. As expected, the performance of a classifier is related to the CNN used to provide it input features. The better the *father* CNN, the better the *children* classifiers. The resulting Meta-Nets ensembles, taking full advantage of 57 base classifiers' diversity, achieve impressive results: With its 0.17% error rate, Meta-Einstein represents the new state-of-the-art for MNIST, as shown in Table 6. Not only do we improve of 20% the previous best system [48], but also do we outperform human capacity, estimated to be 0.20% [49]. Moreover, this experiment shows the incapacity of averaging to exploit the diversity in the classifiers' set. Its error rate is in fact $\approx 40\%$ higher than the best Meta-Net. We believe the main reason to be the unbalanced set of base classifiers, where very few and precise CNNs come up beside a large number of less accurate shallow networks. In conclusion, the MRG in Fig. 4 gives insights on the decision making process of our best system. As predicted, Meta-Nets represent the central hub of the graph. This because they mediate information coming from all the base classifiers to build an optimal *artificial ecology*. Moreover, it is interesting to see that all traditional classifiers are clustered according to their *father* CNN, *i.e.* the one used to extract feature maps.

4.3. The importance of diversity

We believe one of ours most important conclusion to be the absence of a linear correlation between the accuracy of an algorithm and its probability of being selected for an optimal ensemble. As it can be observed in Fig. 3, classification hypothesis with *average* accuracy have little influence on the final prediction rule. Instead, classifiers with an accuracy out of 1 standard deviation ($\approx 0.15\%$) from the average are fundamental for the entire *artificial ecology*.

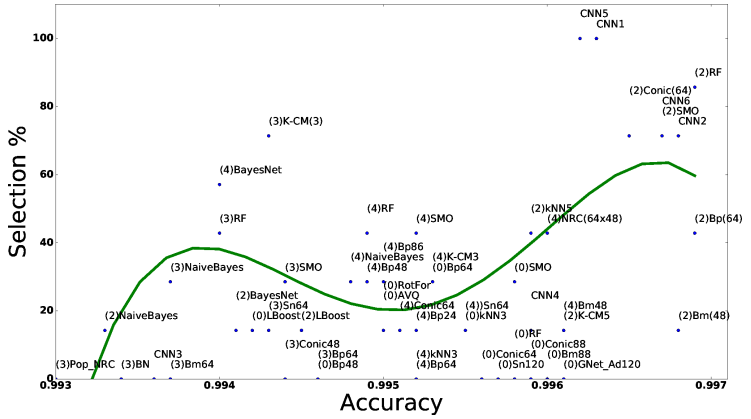

Figure 3: **Base Classifiers Selection in Exp. IV.** In the above plots, we present the correlation between the percentage of times a classifier is selected by Meta-Net to build an ensemble, and its accuracy. Each blue dot represents a base classifier, while the green curve is a 5-th degree polynomial fitting to the points. Its behaviour indicates that hypothesis with average accuracy give little contribution to the creation of a performing classification committee.

This leads us to the point that for the creation of a performing ensemble, two types of hypothesis are necessary. The first are highly accurate, and make the whole ensemble precise. The second have lower accuracy but provide *orthogonality* of thoughts to the final decision, hence giving robustness to the classification [9].

Consequently *we empirically confirmed diversity to be the key for success in decision making*, showing it to have in a learning system the same importance it entails for a biological one.

4.4. State-of-the-art Comparison

Our system achieves incredibly good performance when compared to state-of-the-art methods, as shown in Table 7. In fact, we are the first to beat human performance on the same task, estimated to be $\approx 0.2\%$ [49].

Apart from the extremely low error rate, consisting in only 17 errors out of $10K$ test samples, our methodology is also fully generalizable. In fact, as opposed to systems in [48] and [50], we can directly apply our ensemble pipeline to increase the performance of any CNN structure, without even retraining. This will come at a minimum cost in terms of training and testing times. For example, in our experiments, training 20 shallow networks took almost 2hrs, while the Meta-Nets only took 10 minutes to train, on an Intel i-7 with 32 GB RAM.

5. Conclusions

In this paper, we have presented a novel approach for successful and robust hand-written digit recognition, which achieves astonishing results on the benchmark public dataset MNIST. This was done through our Meta-Nets algorithms, able to create a smart and flexible parliament of classifiers. The members of these ensembles are both

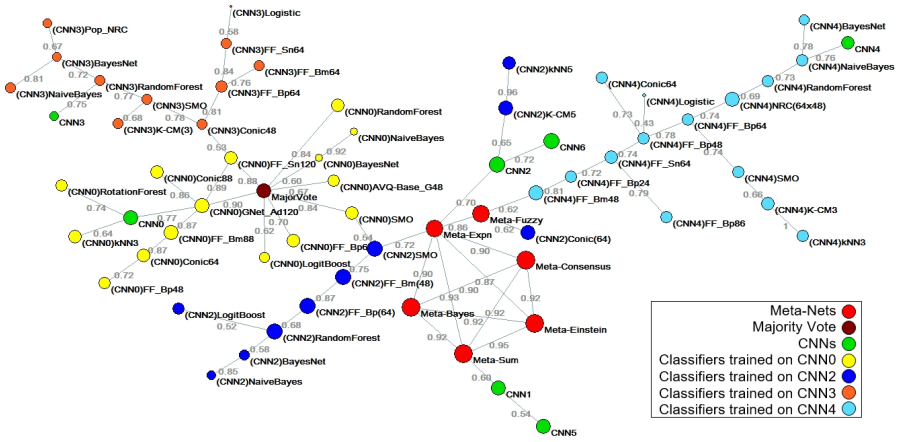

Figure 4: **Exp. IV ErrorMap** In the above MRGs, each node represents a classification method, while the edge weights indicate the relationship's strength between nodes. These are calculated using the methodology explained in Sec. 3.3. To allow a better understanding, the size of the vertices has been drawn in proportion to the accuracy obtained by each method. For the sake of brevity, we report only the MRG of the last experiment.

MNIST						
Method	[1]	[51]	[50]	[2]	[48]	Ours
Error Rate	0.53%	0.29%	0.24%	0.23%	0.21%	**0.17**%

Table 7: **State-of-the-art comparison**: Our methodology establishes the new state-of-the-art result on MNIST. Moreover, its high generalization ability makes it a promising direction for future research in image classification and related tasks.

CNNs and other traditional classification methods, trained on image descriptors extracted from the CNNs' themselves. Apart from the complete Independence of the resulting parliament by the members methodology or accuracy, Meta-Nets can also take full advantage of the diversity in their hypothesis. Surprisingly, we noticed that even less accurate hypothesis are fundamental to build a performing *Computational-Diversity*, showing that in decision making the orthogonality of opinions is as important as their precision.

While motivated by the image classification scenario, the proposed methodology is of interest to a much wider audience as it can be understood as a general technique for improving performance of numerous retrieval and classification related tasks.

Appendix A. Innovative algorithms

Some of the algorithms we used in our experiments are little known or even unpublished. In this section, we want to briefly explain their methodology. The algorithms we will introduce are K-CM, Bimodal Net, Supervised NRC, Gauss Net, Conic Net and Sine Net. All of these were designed by Semeion Research Centre.

Hereafter we will suppose to deal with a database with N variables and M records. The n index will indicate the epoch.

Appendix A.1. K-CM

K-CM [40] and [41] is a supervised neural network, largely used in the field of pattern recognition, based on a contractive principle. K-CM takes advantage of Auto-CM [47], an unsupervised neural network also designed at Semeion, able to explain the hidden relationships among variables, and k-NN classifier [23], [24] and [25]. In the first phase Auto-CM learns the dataset and generates the connection weights matrix $\mathbf{w}$. In the second phase the Auto-CM weights contribute to determining a new fuzzy dataset $\mathbf{Z}$ according to the equation (A.1), where x_{ij} corresponds to the original record and C is the *contraction constant* used by Auto-CM.

$$z_{ij} = x_{ij} \cdot \left(1 - \frac{1}{C^2} \cdot \sum_{k=1}^{N} x_{ik} \left(1 - \frac{w_{jk}^{[Acm]}}{C} \right) \right) \tag{A.1}$$

In the third phase, the k-NN algorithm is used to classify a new pattern $\mathbf{x}_m$ computing the euclidean distance between the mapping $\mathbf{z}_m$ of the test sample and the Z-transformed dataset as shown in the equation (A.2) in order to identify the k nearest neighbors.

$$d_{mi} = \sqrt{\sum_{j=1}^{N} (z_{mj} - z_{ij})^2} \tag{A.2}$$

Where:

$$z_{mj} = x_{mj} \cdot \left(1 - \frac{1}{C^2} \cdot \sum_{k=1}^{N} x_{mk} \left(1 - \frac{w_{jk}^{[Acm]}}{C} \right) \right) \quad \text{with } k \neq j$$

Appendix A.2. Bimodal Net

Bimodal [37] is a supervised neural network characterized by a learning rule that is a combination of gradient descent and vector quantization learning strategies. As shown in Fig. A.5, the input vectors are encoded by the hidden layer where each node consists of two sub-nodes. The sub-nodes are fully-connected with input layer and each of them learn by one of two strategies. The outputs of each couple of sub-nodes are then combined according to the following rules in a single value u_i^h, corresponding to the hidden node output:

$$Qual_i = \frac{1}{1 + e^{-Net_i}} \qquad where \qquad Net_i = \sum_{j}^{N} u_j \cdot w_{ij}^{Q^+} + \theta_i \tag{A.3}$$

$$Quant_i = \left(1 - \frac{\sqrt{d_i}}{N} \right) \cdot e^{\left(-\frac{\sqrt{d_i}}{N} \right)} \qquad where \qquad d_i = \sum_{j}^{N} \left(u_j - w_{ij}^{(Q^-)} \right)^2 \tag{A.4}$$

$$u_i^h = \sqrt{Qual_i^2 + Quant_i^2} \tag{A.5}$$

This new learning strategy can be applied to many different architectures.

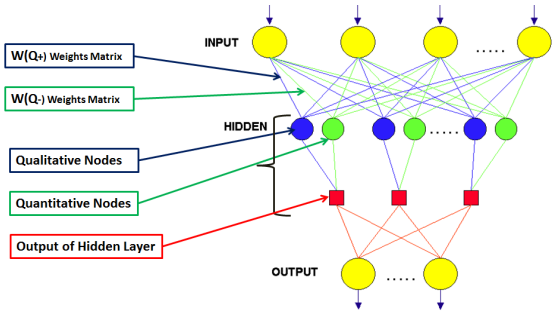

Figure A.5: **Bimodal architecture**

Appendix A.3. Supervised NRC

New Recirculation Neural Network [42] was designed as an unsupervised Auto-Associative Neural Network. Recently it was shown to achieve excellent results even in the supervised version. We present the unpublished SV-NRC for the first time here.

The NRC learns by reasoning through its own learning process. Its output is a weighted average of the real input and of how much the net learns during the previous step. The transfer equations are the following:

$$a_i^{OR} = \frac{1}{1+e^{-Net_i^{OR}}} \qquad where \quad Net_i^{OR} = \sum_{j=1}^{N} w_{ij_{(n)}} \cdot a_j^{IR} + \theta_{i_{(n)}} \tag{A.6}$$

$$a_j^{II} = r \cdot a_j^{IR} + (1-r) \cdot Net_j^{II} \qquad where \quad Net_j^{II} = \sum_{i=1}^{N} w_{ji_{(n)}} \cdot a_i^{OR} + \theta_{j_{(n)}} \tag{A.7}$$

$$a_i^{OI} = r \cdot a_i^{OR} + (1-r) \cdot \frac{1}{1+e^{-Net_i^{OI}}} \qquad where \quad Net_i^{OI} = \sum_{j=1}^{N} w_{ij_{(n)}} \cdot a_j^{II} + \theta_{i_{(n)}} \tag{A.8}$$

Starting from the Real Input $\mathbf{a}^{IR}$, the NRC computes all the values $\mathbf{a}^{OR}$ of the first hidden layer (Real Output) and then the values $\mathbf{a}^{II}$ (Imaginary Input). Lastly all the $\mathbf{a}^{OI}$ (Imaginary Output) values are computed.

Through different modulations of the r parameter it is possible to change the influence of the learning occurred in the previous step.

Supervised NRC is a 3-layer perceptron whose hidden layer corresponds to the first NRC hidden layer, as shown in Fig. A.6. SV-NRC produces its output following the usual sigmoid activation function.

Appendix A.4. Gauss Net

The Gauss Net [39] architecture is the same as a multi-layer perceptron. The special feature of this network lies in the transfer equations, where the following quantities are

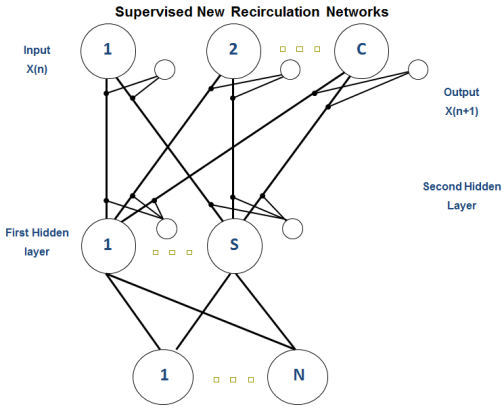

Figure A.6: **Supervised NRC architecture**

computed:

$$d_i^{[n]} = \sqrt{\frac{1}{N} \cdot \sum_j^N \left(input_j^{[n]} - w_{ij} \right)^2} \tag{A.9}$$

$$Net_i^{[n]} = \frac{1}{N} \cdot \sum_j^N input_j^{[n]} \cdot w_{ij} \tag{A.10}$$

$$G_i^{[n]} = Net_i^{[n]} - d_i^{[n]} \tag{A.11}$$

The hidden layer activation function is given by $h_i^{[n]} = e^{-\frac{(G_i^{[n]})^2}{\sigma_i^{[n]}}}$ where $\sigma_i = |d_i^{[n]} + Net_i|$. Gauss Net is still unpublished, we submit it for the first time because of its groundbreaking results.

Appendix A.5. Conic Net

ConicNet [38] is a supervised neural network having the same architecture of a multi-layer perceptron but with a different hidden layers structure as can be observed in Fig. A.7. Each hidden unit is composed of three sub-nodes, two of which, named X and Y, are fully-connected with the input layer while the third is connected to the others by means of internal connections. The outputs of all the sub-nodes are joined in a quadratic equation $\Gamma(X,Y) = aX^2 + 2bXY + cY^2 + 2dX + 2eY + f$. In order to obtain the overall output of the node a non-linear function is applied on $\Gamma(X,Y)$. We remark that the sub-nodes X and Y, connected to the input layer, use two different learning strategies: gradient descent and vector quantization.

Appendix A.6. Sine Net

Sine-Net [43], [44] and [45] is a family of neural networks. The special feature of these networks consists in a double non-linear transformation. The output of each

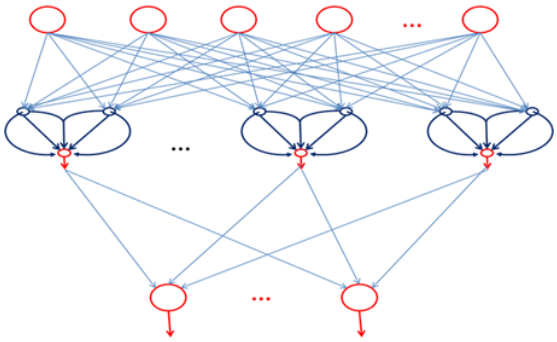

Figure A.7: **Conic Net topology**

node is determined from the equation $x_j^{[s]} = F(G(x_i^{[s-1]}, w_{ji}^{[s]}))$ where $F(\cdot)$ and $G(\cdot)$ are both non-linear applications and s is the layer. The Sine Net name comes from the $G(\cdot)$ function corresponding to the sum of sine curves.

References

References

[1] Y. LeCun, B. Boser, J. S. Denker, D. Henderson, R. E. Howard, W. Hubbard, L. D. Jackel, Backpropagation applied to handwritten zip code recognition, Neural computation 1 (4) (1989) 541–551.

[2] D. CireşAn, U. Meier, J. Masci, J. Schmidhuber, Multi-column deep neural network for traffic sign classification, Neural Networks 32 (2012) 333–338.

[3] M. Buscema, W. J. Tastle, S. Terzi, Meta Net: A New Meta-Classifier Family, Springer, 2013.

[4] J. Schmidhuber, Deep learning in neural networks: An overview, Neural Networks 61 (2015) 85–117.

[5] A. Babenko, V. Lempitsky, Aggregating local deep features for image retrieval, in: IEEE ICCV, 2015, pp. 1269–1277.

[6] A. Sharif Razavian, H. Azizpour, J. Sullivan, S. Carlsson, Cnn features off-the-shelf: an astounding baseline for recognition, in: IEEE CVPR Workshops, 2014, pp. 169–177.

[7] E. Simo-Serra, E. Trulls, L. Ferraz, I. Kokkinos, P. Fua, F. Moreno-Noguer, Discriminative learning of deep convolutional feature point descriptors, in: (ICCV), 2015, pp. 483–498.

[8] J. Zbontar, Y. LeCun, Computing the stereo matching cost with a convolutional neural network, in: Proceedings of the IEEE Conference on Computer Vision and Pattern Recognition, 2015, pp. 1592–1599.

[9] A. Krogh, J. Vedelsby, et al., Neural network ensembles, cross validation, and active learning.

[10] L. Breiman, Bagging predictors, Machine learning 24 (2) (1996) 123–140.

[11] M. Buscema, P. L. Sacco, Guacamole: A new paradigm for unsupervised competitive learning, in: Data Mining Applications Using Artificial Adaptive Systems, Springer, 2013, pp. 211–230.

[12] Y. Freund, R. E. Schapire, A desicion-theoretic generalization of on-line learning and an application to boosting, in: European conference on computational learning theory, Springer Berlin Heidelberg, 1995, pp. 23–37.

[13] R. Girshick, J. Donahue, T. Darrell, J. Malik, Rich feature hierarchies for accurate object detection and semantic segmentation, in: Proceedings of the IEEE conference on CVPR, 2014, pp. 580–587.

[14] M. D. Zeiler, R. Fergus, Visualizing and understanding convolutional networks, in: European Conference on Computer Vision, Springer, 2014, pp. 818–833.

[15] T. Kohonen, Improved versions of learning vector quantization, in: Neural Networks, 1990., 1990 IJCNN International Joint Conference on, IEEE, 1990, pp. 545–550.

[16] K. Bart, Neural networks and fuzzy systems: A dynamical systems approach to machine intelligence, Pren-tice-Hall, Englewood Cliffs.

[17] B. Kosko, Neural networks for signal processing, Prentice-Hall, Inc., 1992.

[18] M. Buscema, L. Catzola, AVQ1 Basic and AVQ2 Advanced, Semeion Report.

[19] S. H. Nielsen, T. D. Nielsen, Adapting bayes network structures to non-stationary domains, International Journal of Approximate Reasoning 49 (2) (2008) 379–397.

[20] N. Friedman, D. Geiger, M. Goldszmidt, Bayesian network classifiers, Machine learning 29 (2-3) (1997) 131–163.

[21] D. E. Rumelhart, G. E. Hinton, R. J. Williams, Learning internal representations by error propagation, Parallel Distribuited Processing 1 (1986) 318–362.

[22] M. Buscema, Back propagation neural networks, Substance use & misuse 33 (2) (1998) 233–270.

[23] T. Cover, P. Hart, Nearest neighbor pattern classification, IEEE transactions on information theory 13 (1) (1967) 21–27.

[24] B. Kowalski, C. Bender, k-nearest neighbor classification rule (pattern recognition) applied to nuclear magnetic resonance spectral interpretation, Analytical Chemistry 44 (8) (1972) 1405–1411.

[25] D. W. Aha, D. Kibler, M. K. Albert, Instance-based learning algorithms, Machine learning 6 (1) (1991) 37–66.

[26] S. Le Cessie, J. C. Van Houwelingen, Ridge estimators in logistic regression, Applied statistics (1992) 191–201.

[27] D. W. Hosmer, S. Lemeshow, Interpretation of the fitted logistic regression model, Applied Logistic Regression, Second Edition (2000) 47–90.

[28] G. H. John, P. Langley, Estimating continuous distributions in bayesian classifiers, in: Proceedings of the Eleventh conference on Uncertainty in artificial intelligence, Morgan Kaufmann Publishers Inc., 1995, pp. 338–345.

[29] H. Zhang, The optimality of naive bayes, AA 1 (2) (2004) 3.

[30] I. Rish, An empirical study of the naive bayes classifier, in: IJCAI 2001 workshop on empirical methods in artificial intelligence, Vol. 3, IBM New York, 2001, pp. 41–46.

[31] L. Breiman, Random forests, Machine learning 45 (1) (2001) 5–32.

[32] J. Quinlan, C4. 5: Programs for machine learning. c4. 5-programs for machine learning/j. ross quinlan (1993).

[33] J. Platt, Fast training of support vector machines using sequential minimal optimization, in: B. Schoelkopf, C. Burges, A. Smola (Eds.), Advances in Kernel Methods - Support Vector Learning, MIT Press, 1998, pp. 10–27.

[34] S. S. Keerthi, S. K. Shevade, C. Bhattacharyya, K. R. K. Murthy, Improvements to platt's smo algorithm for svm classifier design, Neural computation 13 (3) (2001) 637–649.

[35] S. S. Keerthi, E. G. Gilbert, Convergence of a generalized smo algorithm for svm classifier design, Machine Learning 46 (1-3) (2002) 351–360.

[36] V. Kecman, Learning and soft computing: support vector machines, neural networks, and fuzzy logic models, MIT press, 2001.

[37] M. Buscema, Reti Neurali Artificiali per l'orientamento professionale, Franco Angeli, Semeion Reading, Milano, 2004, Ch. 9, pp. 179–180.

[38] P. M. Buscema, G. Massini, M. Fabrizi, M. Breda, The anns approach to dem reconstruction, submitted to Computational Intelligence.

[39] P. M. Buscema, Gauss-net, Mimeo, Semeion Research Center of Sciences of Communication.

[40] M. Buscema, V. Consonni, D. Ballabio, A. Mauri, G. Massini, M. Breda, R. Todeschini, K-CM: A new artificial neural network. application to supervised pattern recognition, Chemometrics and Intelligent Laboratory Systems 138 (2014) 110–119.

[41] M. Gironi, B. Borgiani, E. Farina, E. Mariani, C. Cursano, M. Alberoni, R. Nemni, G. Comi, M. Buscema, R. Furlan, et al., A global immune deficit in alzheimer's disease and mild cognitive impairment disclosed by a novel data mining process, Journal of Alzheimer's Disease 43 (4) (2015) 1199–1213.

[42] M. Buscema, Recirculation neural networks, Substance use & misuse 33 (2) (1998) 383–388.

[43] M. Buscema, S. Terzi, M. Breda, Using sinusoidal modulated weights improve feed-forward neural network performances in classification and functional approximation problems.., WSEAS Transactions on information science and applications 3 (5) (2006) 885–893.

[44] M. Buscema, M. Breda, S. Terzi, A feed forward sine based neural network for functional approximation of a waste incinerator emissions, in: Proceedings of the 8th WSEAS international conference on automatic control, modeling and simulation, Prague, 2006.

[45] P. M. Buscema, Sine net: an artificial neural network. applicant semeion research centre, european Patent (Application n. 03425582.8 deposited 09-09-2003). USA Patent No US 7,788,196 B2 - Aug. 31, 2010. International Patent: Application PCT/EP2004/05189 deposited 08-28-2004.

[46] M. Buscema, Genetic doping algorithm (gend): theory and applications, Expert Systems 21 (2) (2004) 63–79.

[47] M. Buscema, P. L. Sacco, Auto-contractive maps, the h function, and the maximally regular graph (mrg): A new methodology for data mining, in: Applications of mathematics in models, artificial neural networks and arts, Springer, 2010, pp. 227–275.

[48] L. Wan, M. Zeiler, S. Zhang, Y. L. Cun, R. Fergus, Regularization of neural networks using dropconnect, in: Proceedings of the 30th International Conference on Machine Learning (ICML-13), 2013, pp. 1058–1066.

[49] Y. LeCun, L. Jackel, C. Cortes, et al., Learning algorithms for classification: A comparison on handwritten digit recognition.

[50] J.-R. Chang, Y.-S. Chen, Batch-normalized maxout network in network, arXiv preprint arXiv:1511.02583.

[51] C.-Y. Lee, P. W. Gallagher, Z. Tu, Generalizing pooling functions in convolutional neural networks: Mixed, gated, and tree.